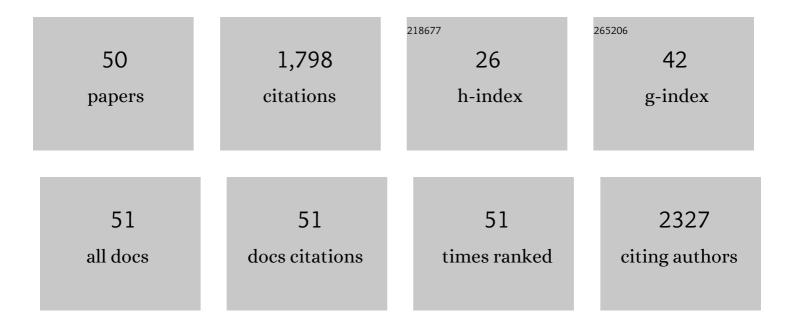
Joseph A Spernyak

List of Publications by Year in descending order

Source: https://exaly.com/author-pdf/4813060/publications.pdf Version: 2024-02-01



#	Article	IF	CITATIONS
1	Metalâ^'Organic Polyhedron with Four Fe(III) Centers Producing Enhanced T ₁ Magnetic Resonance Imaging Contrast in Tumors. Inorganic Chemistry, 2022, 61, 2603-2611.	4.0	14
2	A mitochondrial unfolded protein response inhibitor suppresses prostate cancer growth in mice via HSP60. Journal of Clinical Investigation, 2022, 132, .	8.2	21
3	Tumor-Avid 3-(1â€2-Hexyloxy)ethyl-3-devinylpyrpyropheophorbide-a (HPPH)-3Gd(III)tetraxetan (DOTA) Conjugate Defines Primary Tumors and Metastases. Journal of Medicinal Chemistry, 2022, 65, 9267-9280.	6.4	3
4	Fast Stereolithography Printing of Large‣cale Biocompatible Hydrogel Models. Advanced Healthcare Materials, 2021, 10, e2002103.	7.6	48
5	3D Bioprinting: Fast Stereolithography Printing of Large‣cale Biocompatible Hydrogel Models (Adv.) Tj ETQq1	1 9.78431	14 ₁ gBT /Ove
6	Dinuclear Fe(III) Hydroxypropyl-Appended Macrocyclic Complexes as MRI Probes. Inorganic Chemistry, 2021, 60, 8651-8664.	4.0	24
7	Small Endogeneous Peptide Mitigates Myocardial Remodeling in a Mouse Model of Cardioselective Galectin-3 Overexpression. Circulation: Heart Failure, 2021, 14, e008510.	3.9	8
8	Comparison of phosphonate, hydroxypropyl and carboxylate pendants in Fe(III) macrocyclic complexes as MRI contrast agents. Journal of Inorganic Biochemistry, 2021, 225, 111594.	3.5	11
9	Liposomal Fe(III) Macrocyclic Complexes with Hydroxypropyl Pendants as MRI Probes. ACS Applied Bio Materials, 2021, 4, 7951-7960.	4.6	9
10	Human wildtype tau expression in cholinergic pedunculopontine tegmental neurons is sufficient to produce PSPâ€like behavioural deficits and neuropathology. European Journal of Neuroscience, 2021, 54, 7688-7709.	2.6	6
11	A Class of Fe ^{III} Macrocyclic Complexes with Alcohol Donor Groups as Effective <i>T</i> ₁ MRI Contrast Agents. Angewandte Chemie - International Edition, 2020, 59, 2414-2419.	13.8	49
12	Isomeric Co(ii) paraCEST agents as pH responsive MRI probes. Dalton Transactions, 2020, 49, 279-284.	3.3	12
13	A Class of Fe ^{III} Macrocyclic Complexes with Alcohol Donor Groups as Effective <i>T</i> ₁ MRI Contrast Agents. Angewandte Chemie, 2020, 132, 2435-2440.	2.0	20
14	Saccharomyces cerevisiae and Candida albicans Yeast Cells Labeled with Fe(III) Complexes as MRI Probes. Magnetochemistry, 2020, 6, 41.	2.4	0
15	The Structures of Gd(III) Chelates Conjugated at the Periphery of 3â€(1'â€Hexyloxy)ethylâ€3â€devinylpyropheophorbideâ€a (HPPH) Have a Significant Impact on the Imaging Therapy of Cancer. ChemMedChem, 2020, 15, 2058-2070.	a s d2	11
16	Modulating the Properties of Fe(III) Macrocyclic MRI Contrast Agents by Appending Sulfonate or Hydroxyl Groups. Molecules, 2020, 25, 2291.	3.8	29
17	MRI and fluorescence studies of Saccharomyces cerevisiae loaded with a bimodal Fe(III) T1 contrast agent. Journal of Inorganic Biochemistry, 2019, 201, 110832.	3.5	15
18	Irradiance controls photodynamic efficacy and tissue heating in experimental tumours: implication for interstitial PDT of locally advanced cancer. British Journal of Cancer, 2018, 119, 1191-1199.	6.4	33

JOSEPH A SPERNYAK

#	Article	IF	CITATIONS
19	A Small Peptide Ac-SDKP Inhibits Radiation-Induced Cardiomyopathy. Circulation: Heart Failure, 2018, 11, e004867.	3.9	28
20	MnO ₂ Nanotube-Based NanoSearchlight for Imaging of Multiple MicroRNAs in Live Cells. ACS Applied Materials & Interfaces, 2017, 9, 23325-23332.	8.0	33
21	Multifunctional Liposomes for Imageâ€Guided Intratumoral Chemoâ€Phototherapy. Advanced Healthcare Materials, 2017, 6, 1700253.	7.6	46
22	Design of Hydrated Porphyrin-Phospholipid Bilayers with Enhanced Magnetic Resonance Contrast. Small, 2017, 13, 1602505.	10.0	18
23	Gear Up for a pH Shift: A Responsive Iron(II) 2-Amino-6-picolyl-Appended Macrocyclic paraCEST Agent That Protonates at a Pendent Group. Inorganic Chemistry, 2016, 55, 12001-12010.	4.0	45
24	Six, Seven or Eight Coordinate Fe ^{II} , Co ^{II} or Ni ^{II} Complexes of Amideâ€Appended Tetraazamacrocycles for ParaCEST Thermometry. Chemistry - A European Journal, 2015, 21, 18290-18300.	3.3	42
25	Seven-Coordinate Co ^{II} , Fe ^{II} and Six-Coordinate Ni ^{II} Amide-Appended Macrocyclic Complexes as ParaCEST Agents in Biological Media. Inorganic Chemistry, 2014, 53, 8311-8321.	4.0	43
26	A Redoxâ€Activated MRI Contrast Agent that Switches Between Paramagnetic and Diamagnetic States. Angewandte Chemie - International Edition, 2013, 52, 13997-14000.	13.8	95
27	CoCEST: cobalt(ii) amide-appended paraCEST MRI contrast agents. Chemical Communications, 2013, 49, 10025.	4.1	77
28	Potent Effects Of The Vascular Disrupting Agent, ASA404 (DMXAA) On The Marrow Microenvironment In Preclinical Human Leukemia and Lymphoma Models. Blood, 2013, 122, 3953-3953.	1.4	1
29	The NiCEST Approach: Nickel(II) ParaCEST MRI Contrast Agents. Journal of the American Chemical Society, 2012, 134, 18503-18505.	13.7	79
30	Mechanisms of Tumor Vascular Priming by a Nanoparticulate Doxorubicin Formulation. Pharmaceutical Research, 2012, 29, 3312-3324.	3.5	14
31	Iron(II) PARACEST MRI Contrast Agents. Journal of the American Chemical Society, 2011, 133, 14154-14156.	13.7	108
32	Mild Elevation of Body Temperature Reduces Tumor Interstitial Fluid Pressure and Hypoxia and Enhances Efficacy of Radiotherapy in Murine Tumor Models. Cancer Research, 2011, 71, 3872-3880.	0.9	105
33	Peroxiredoxin 1 Controls Prostate Cancer Growth through Toll-Like Receptor 4–Dependent Regulation of Tumor Vasculature. Cancer Research, 2011, 71, 1637-1646.	0.9	98
34	Anti-Vascular and Anti-Tumor Effects of the Vascular Disrupting Agent ASA404 (DMXAA) in Human Acute Leukemia Xenograft Models. Blood, 2011, 118, 4293-4293.	1.4	0
35	Hexylether Derivative of Pyropheophorbide-a (HPPH) on Conjugating with 3Gadolinium(III) Aminobenzyldiethylenetriaminepentaacetic Acid Shows Potential for in Vivo Tumor Imaging (MR,) Tj ETQq1 1 0	.78 4 3d 4 rg	BT4@verlock
36	Synthesis of Tumor-Avid Photosensitizerâ^'Gd(III)DTPA Conjugates: Impact of the Number of Gadolinium Units in T1/T2 Relaxivity, Intracellular localization, and Photosensitizing Efficacy. Bioconjugate Chemistry, 2010, 21, 816-827.	3.6	35

JOSEPH A SPERNYAK

#	Article	IF	CITATIONS
37	The Vps33a gene regulates behavior and cerebellar Purkinje cell number. Brain Research, 2009, 1266, 18-28.	2.2	22
38	Performance of a novel piezoelectric motor at 4.7 T: applications and initial tests. Magnetic Resonance Imaging, 2008, 26, 426-432.	1.8	12
39	Magnetic resonance imaging and spectroscopy in a mouse model of schizophrenia. Brain Research Bulletin, 2008, 75, 556-561.	3.0	5
40	Light Delivery over Extended Time Periods Enhances the Effectiveness of Photodynamic Therapy. Clinical Cancer Research, 2008, 14, 2796-2805.	7.0	66
41	Genetically Altered Expression of Spermidine/Spermine N1-Acetyltransferase Affects Fat Metabolism in Mice via Acetyl-CoA. Journal of Biological Chemistry, 2007, 282, 8404-8413.	3.4	120
42	Visualizing the Acute Effects of Vascular-Targeted Therapy In Vivo Using Intravital Microscopy and Magnetic Resonance Imaging: Correlation with Endothelial Apoptosis, Cytokine Induction, and Treatment Outcome. Neoplasia, 2007, 9, 128-135.	5.3	40
43	Brain MR Imaging and Proton MR Spectroscopy in Female Mice with Pyruvate Dehydrogenase Complex Deficiency. Neurochemical Research, 2007, 32, 645-654.	3.3	11
44	Activity of the Vascular-Disrupting Agent 5,6-Dimethylxanthenone-4-Acetic Acid against Human Head and Neck Carcinoma Xenografts. Neoplasia, 2006, 8, 534-542.	5.3	31
45	Ventricular size mapping in a transgenic model of schizophrenia. Developmental Brain Research, 2005, 154, 35-44.	1.7	19
46	Tumor Vascular Response to Photodynamic Therapy and the Antivascular Agent 5,6-Dimethylxanthenone-4-Acetic Acid: Implications for Combination Therapy. Clinical Cancer Research, 2005, 11, 4241-4250.	7.0	60
47	High Correlation of Whole-Body Red Fluorescent Protein Imaging and Magnetic Resonance Imaging on an Orthotopic Model of Pancreatic Cancer. Cancer Research, 2005, 65, 9829-9833.	0.9	48
48	Chlorophyll-a Analogues Conjugated with Aminobenzyl-DTPA as Potential Bifunctional Agents for Magnetic Resonance Imaging and Photodynamic Therapy. Bioconjugate Chemistry, 2005, 16, 32-42.	3.6	64
49	Lack of Microvessels in Well-Differentiated Regions of Human Head and Neck Squamous Cell Carcinoma A253 Associated with Functional Magnetic Resonance Imaging Detectable Hypoxia, Limited Drug Delivery, and Resistance to Irinotecan Therapy. Clinical Cancer Research, 2004, 10, 8005-8017.	7.0	47
50	High-resolution magnetic resonance imaging of the efficacy of the cytosine analogue 1-[2-C-cyano-2-deoxy-beta-D-arabino-pentofuranosyl]-N(4)-palmitoyl cytosine (CS-682) in a liver-metastasis athymic nude mouse model. Cancer Research, 2003, 63, 2477-82.	0.9	12